Materials Characterization 141 (2018) 406–411

Contents lists available at ScienceDirect

Materials Characterization

journal homepage: www.elsevier.com/locate/matchar

Approximate icosahedral symmetry of α-*Al(Fe,Mn,Cr)Si* in electron backscatter diffraction analysis of a secondary Al-Si casting alloy

Hanka Becker, Andreas Leineweber*

TU Bergakademie Freiberg, Institute of Materials Science, Gustav-Zeuner Straße 5, 09599 Freiberg, Germany

ARTICLE INFO

Keywords:
Solidification microstructure
Electron backscattering diffraction (EBSD)
Aluminum alloys
Quasicrystalline approximant
Pseudosymmetry
Intermetallic morphology

ABSTRACT

Frequent systematic misindexing of electron backscatter diffraction patterns with five differently oriented pseudosymmetric solutions was observed for the cubic α-*Al(Fe,M)Si* phase with *M* = Mn, Cr encountered in secondary Al-Si casting alloy. That misindexing can be ascribed to the close structural relationship of the cubic crystal structure of α-*Al(Fe,M)Si* to that of the corresponding icosahedral quasicrystal. Robust identification of the correct among the five nearby solutions during automatic indexing can be achieved, which sensitively depends on the accuracy of Kikuchi-band detection applying Hough-space related indexing methods. Based on the correct crystallographic orientation solution, facets of the particles with bulk polyhedral and Chinese script morphology were determined to be {110} planes. Likewise, the habit planes of the α-*Al(Fe,M)Si* phase particles located at the naturally occurring oxide film are {110} planes.

1. Introduction

Iron is the main metallic impurity element in secondary Al-Si casting alloys. Its presence can lead to the formation of Fe-containing intermetallic phases, in particular the α and the β phase. The β-$Al_{4.5}FeSi$ phase [1] appears with plate-like shape being detrimental on the mechanical properties [2–4] by acting as regions for stress concentration. Moreover, the β phase plates may hinder effective feeding by blocking liquid metal resulting in shrinkage porosity [5–10]. Therefore, much effort was dedicated to promote the formation of the α phase with generally less detrimental morphologies, e.g. the Chinese script morphology, than shown by the β phase e.g. by addition of *M* = Mn, Cr [4,8,11–19]. For the aim of Fe removal from secondary Al-Si casting alloys by separation of melt from primary Fe containing α phase, the formation of primary α phase in bulk polyhedral shape is promoted [20–24]. Furthermore, the α phase can evolve by reactive diffusion during bonding of cast iron or steel and Al-Si alloys [25,26].

In pure Al-Si-Fe alloys, the *hexagonal α-AlFeSi* phase (also α_h) with a composition given by $Al_{7.1}Fe_2Si$ is hexagonal with space group $P6_3/mmc$ [27]. However, in presence of as small amounts as > 0.03 wt% Cr [28] or > 0.3 wt% Mn [28–30] the *cubic* α-*Al(Fe,M)Si* phase (also α_c) forms with approximate compositions between $Al_{20}(Fe,M)_5Si_2$ [31] and $Al_{15}(Fe,M)_3Si_2$ [32]. It has space group $Im\bar{3}$ at low *M*/Fe ratios or $Pm\bar{3}$ at high *M*/Fe ratios [31,33], leading, however, to very minor differences in the diffraction effects. Depending on the external conditions, e.g. elemental concentration and cooling rate [13], the cubic α-*Al(Fe,M)Si* phase evolves into a fascinating variety of morphologies during co-eutectic solidification and during primary crystallization (Chinese script, bulk facetted polyhedra etc.) [13,34]. From these morphologies growth mechanisms have been proposed [13,34,35]. Furthermore, favored heterogeneous nucleation of the α phase on various nucleating surfaces and on the naturally occurring oxide film of Al alloys [36–39] was reported. Suitable match planes were discussed between the α phase [36]. However, crystallographic orientation data based verification, e.g. by electron backscatter diffraction (EBSD), of the growth morphologies or orientation relationships to nucleating surfaces is not available yet.

The present investigation scrutinizes the indexing peculiarities of electron backscatter diffraction patterns (EBSP) of the cubic α-*Al(Fe,M)Si* phase with respect to the specifics of its crystal structure. The understanding of the origin of these peculiarities in automatic EBSD indexing is the basis to access the correct orientation information in order to investigate the growth morphology of the α-*Al(Fe,M)Si* phase. The growth morphology of bulk polyhedral particles of the α-*Al(Fe,M)Si* phase was statistically evaluated based on crystallographic orientation data for the first time. It is shown that the Chinese script morphology closely relates to this morphology. The habit plane of the α-*Al(Fe,M)Si* phase particles located towards the naturally occurring oxide film is reported.

* Corresponding author at: Haus Metallkunde/Raum 115/116, Gustav-Zeuner-Straße 5, 09599 Freiberg, Germany.
E-mail addresses: hanka.becker@iww.tu-freiberg.de (H. Becker), andreas.leineweber@iww.tu-freiberg.de (A. Leineweber).
URL: http://tu-freiberg.de/fakult5/iww (A. Leineweber).

https://doi.org/10.1016/j.matchar.2018.05.013
Received 15 March 2018; Received in revised form 2 May 2018; Accepted 8 May 2018
Available online 09 May 2018
1044-5803/

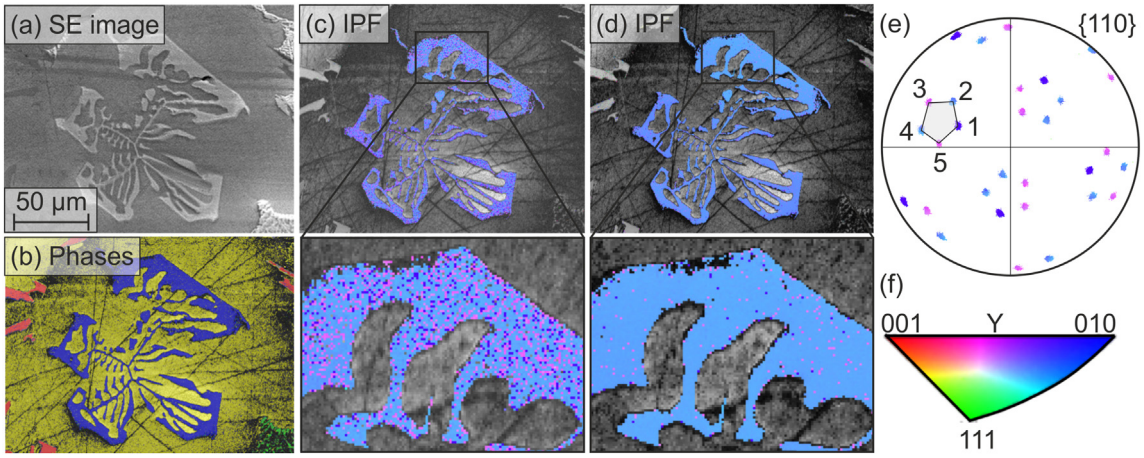

Fig. 1. (a) Secondary electron contrast image of a Chinese-script particle. The corresponding EBSD maps illustrate (b) the phase distribution (Al-yellow, Si-red, Al_2Cu-green, α-*Al(Fe,M)Si*-blue) and the crystallographic orientations of α-*Al(Fe,M)Si* received after applying (c) standard indexing and (d) optimized indexing conditions (see Section 3.3). (e) The {110} pole figure points out the five different orientation solutions appearing in (c) and (d); with probabilities before and after optimization of the indexing procedure 1: 8.0% → 1.0%, 2: 72.7% → 93.2%, 3: 15.9% → 4.5%, 4: 4.3% → 0.6%, 5: 1.1% → 0.6%. (f) Inverse pole figure coloring used in (c), (d) and (e). Dark stripes in the EBSD images are consequence of scratches on the sample surface appearing in ductile Aluminum only. (For interpretation of the references to color in this figure legend, the reader is referred to the web version of this article.)

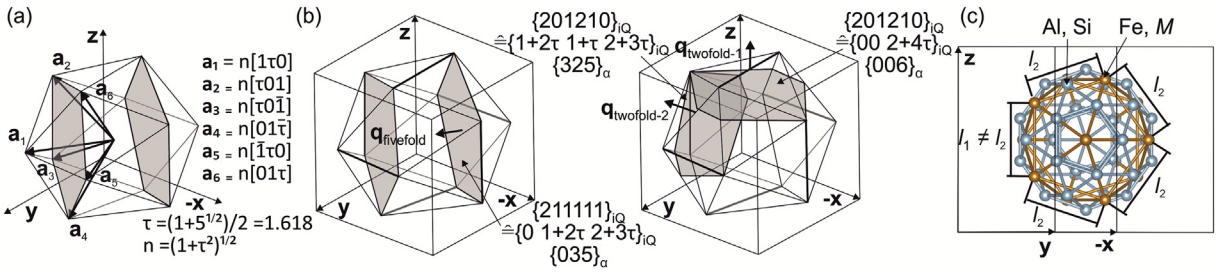

Fig. 2. (a) Basis vectors $\mathbf{a}_{1-6}$ of an icosahedral Quasicrystal (iQ) according to [49]. The lattice planes with diffraction vector parallel to a fivefold axis are indicated. Their relation to Cartesian indices is shown. (b) The diffraction vectors $\mathbf{q}_{\text{fivefold}}$ and $\mathbf{q}_{\text{twofold-1,2}}$ (or near $\mathbf{q}_{\text{fivefold}}$ and near $\mathbf{q}_{\text{twofold-2}}$ in approximant case) and corresponding planes for the iQ and for the α-*Al(Fe,M)Si* phase are exemplarily illustrated. (c) Centered cluster of cubic α-*Al(Fe,M)Si* [31] with viewing direction along one of the almost fivefold $\langle 035\rangle_\alpha$ axes illustrating the approximate icosahedral character of the cluster. l_1 and l_2 indicate the edge length of the cluster. Note, the clusters on the corners and additional atoms filling the space between the clusters are not shown.

Table 1
Indices of reflectors with highest intensity in iQs and the iQ approximant α-*Al(Fe,M)Si*. Note that $2^{-1/2}\{hkl\}_{iQ} \approx \{hkl\}_\alpha$ [50]. $d_{\{hkl\}\alpha}$ is the lattice plane distance of α-*Al(Fe,M)Si* with $a = 12.558$ Å.

iQ			α-*Al(Fe,M)Si*		
6 indices	Multiplicity	3 indices $\{hkl\}_{iQ}$	3 indices $\{hkl\}_\alpha$	Multiplicity	$d_{\{hkl\}\alpha}$ [Å]
$\{211111\}_{iQ}$	6	$\{0\ 1+2\tau\ 2+3\tau\}_{iQ}$	$\{035\}_\alpha$	6	2.154
$\{201210\}_{iQ}$	15	$\{00\ 2+4\tau\}_{iQ}$	$\{006\}_\alpha$	3	2.093
		$\{1+2\tau\ 1+\tau\ 2+3\tau\}_{iQ}$	$\{325\}_\alpha$	12	2.038
$\{302320\}_{iQ}$	15	$\{00\ 4+6\tau\}_{iQ}$	$\{00\ 10\}_\alpha$	3	1.256
		$\{2+3\tau\ 1+2\tau\ 3+5\tau\}_{iQ}$	$\{538\}_\alpha$	12	1.268

2. Experimental

A commercial secondary AlSi9Cu3 alloy with 2.5 wt% Fe was used for investigation of a particle with Chinese script morphology. 0.8 wt% Mn and 0.4 wt% Cr were added to promote formation of α-*Al(Fe,M)Si* instead of the β phase. The melt was treated for 4 h at 620 °C, close above the temperature of beginning solidification of Al, to allow primary formation of α-*Al(Fe,M)Si*. Afterwards the melt was cooled in air. Further details are available in [20]. An Al7.1Si0.9Fe0.6Mn alloy was utilized to study the growth morphology of bulk polyhedral particles. It was prepared in an electric arc furnace from pure elements Fe (AlfaAesar, pieces, 99.99% metals basis) and Al (AlfaAesar, slugs, 99.9999% metals basis), Si (AlfaAesar, pieces, 99.9999% metal basis), Mn (AlfaAesar, pieces, 99.95% metal basis). Neither by weighting nor by EDS significant loss of material was indicated. The sample was fully remelted at 850 °C for 1 h. Subsequent furnace cooling of approx. 1 h duration was applied towards the target temperature of 620 °C. After 2 h at 620 °C, the sample was quenched in water. Microstructural investigations by scanning electron microscopy including EBSD were carried out at the polished (final stage: colloidal silica suspension; OP-S, Struers) cross section of the solidified ingot. A FEG Zeiss LEO 1530 GEMINI equipped with a Nordlys II EBSD detector (Oxford Instruments) and HKL Channel5 software (Oxford instruments) was used. EBSP acquisition was performed at 20 kV in high-current mode with an aperture of 120 µm recording 20 ms per frame and 3 frames per pattern. The EBSPs with size of 336 × 256 pixels were stored for subsequent analysis with different band detection parameters. The initially used standard Hough-space resolution parameter of 50 was altered during subsequent analysis up to the software maximum of 125. All results presented here refer to analysis of Kikuchi-band edges. The used part of the EBSD pattern was kept unchanged during reanalysis. 8 bands per EBSP were detected by the Hough-space method. The positions of 7 of 8 simulated